



# The role of surface-bound hydroxyl radicals in the reaction between H<sub>2</sub>O<sub>2</sub> and UO<sub>2</sub>

Alexandre Barreiro Fidalgo, Yuta Kumagai & Mats Jonsson

To cite this article: Alexandre Barreiro Fidalgo, Yuta Kumagai & Mats Jonsson (2018) The role of surface-bound hydroxyl radicals in the reaction between H<sub>2</sub>O<sub>2</sub> and UO<sub>2</sub>, Journal of Coordination Chemistry, 71:11-13, 1799-1807, DOI: [10.1080/00958972.2018.1466287](https://doi.org/10.1080/00958972.2018.1466287)

To link to this article: <https://doi.org/10.1080/00958972.2018.1466287>



© 2018 The Authors. Published by Informa UK Limited, trading as Taylor & Francis Group



Published online: 09 May 2018.



Submit your article to this journal [↗](#)



Article views: 928



View related articles [↗](#)



View Crossmark data [↗](#)



Citing articles: 13 View citing articles [↗](#)

## The role of surface-bound hydroxyl radicals in the reaction between $\text{H}_2\text{O}_2$ and $\text{UO}_2$

Alexandre Barreiro Fidalgo<sup>a</sup>, Yuta Kumagai<sup>b</sup> and Mats Jonsson<sup>a</sup>

<sup>a</sup>Department of Chemistry, Applied Physical Chemistry, KTH Royal Institute of Technology, Stockholm, Sweden;

<sup>b</sup>Japan Atomic Energy Agency, Nuclear Science and Engineering Directorate, Nakagun, Japan

### ABSTRACT

In this work, we have studied the reaction between  $\text{H}_2\text{O}_2$  and  $\text{UO}_2$  with particular focus on the nature of the hydroxyl radical formed as an intermediate. Experiments were performed to study the kinetics of  $\text{H}_2\text{O}_2$  consumption and uranium dissolution at different initial  $\text{H}_2\text{O}_2$  concentrations. The results show that the consumption rates at a given  $\text{H}_2\text{O}_2$  concentration are different depending on the initial  $\text{H}_2\text{O}_2$  concentration. This is attributed to an alteration of the reactive interface, likely caused by blocking of surface sites by oxidized U/surface-bound hydroxyl radicals. The dissolution yield given by the amount of dissolved uranium divided by the amount of consumed hydrogen peroxide was used to compare the different cases. For all initial  $\text{H}_2\text{O}_2$  concentrations, the dissolution yield increases with reaction time. The final dissolution yield decreases with increasing initial  $\text{H}_2\text{O}_2$  concentration. This is expected from the mechanism of catalytic decomposition of  $\text{H}_2\text{O}_2$  on oxide surfaces. As the experiments were performed in solutions containing 10 mM  $\text{HCO}_3^-$  and a strong concentration dependence was observed in the 0.2–2.0 mM  $\text{H}_2\text{O}_2$  concentration range, we conclude that the intermediate hydroxyl radical is surface bound rather than free.

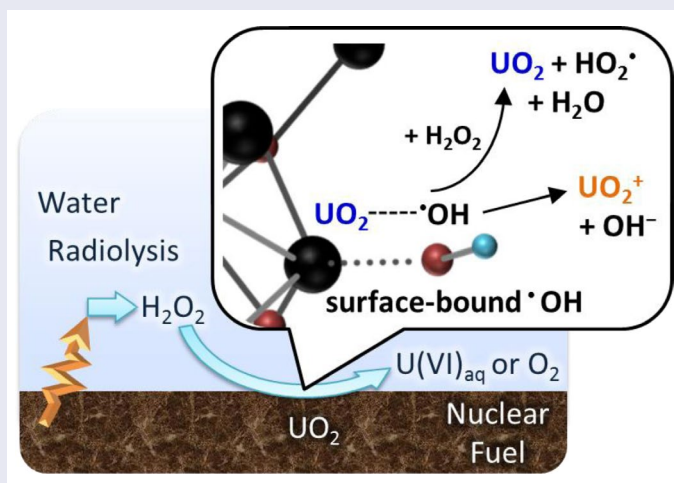
### ARTICLE HISTORY


Received 14 February 2018

Accepted 21 March 2018

### KEYWORDS

Hydroxyl radical;  $\text{H}_2\text{O}_2$ ;  $\text{UO}_2$ ; catalysis; surface



CONTACT Mats Jonsson  matsj@kth.se

© 2018 The Authors. Published by Informa UK Limited, trading as Taylor & Francis Group

This is an Open Access article distributed under the terms of the Creative Commons Attribution-NonCommercial-NoDerivatives License (<http://creativecommons.org/licenses/by-nc-nd/4.0/>), which permits non-commercial re-use, distribution, and reproduction in any medium, provided the original work is properly cited, and is not altered, transformed, or built upon in any way.

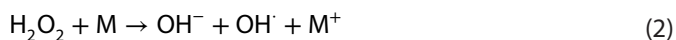
## 1. Introduction

The chemistry of hydrogen peroxide has been studied in detail for more than two centuries and still attracts considerable attention in several fields. Since hydrogen peroxide is produced upon irradiation of water [1], its reactivity is of prime interest for many nuclear technological applications such as water-cooled nuclear reactors, nuclear fuel reprocessing plants and repositories for used nuclear fuel and other types of radioactive waste. The main concern in these cases is corrosion of various materials and the consequences of this. As the consequences of nuclear corrosion can easily be extrapolated to disaster scenarios, it is essential that we fully understand these processes. The materials in contact with the aqueous phases containing radiolytically produced hydrogen peroxide are almost exclusively metal oxides or metals covered by metal oxide. Hence, reactions between hydrogen peroxide and metal oxides are of prime interest. For oxides that can be further oxidized, two types of reactions are possible. The first type of reaction is oxidation of the oxide by hydrogen peroxide and the second type of reaction is catalytical decomposition of  $\text{H}_2\text{O}_2$  on the oxide surface. The latter reaction converts  $\text{H}_2\text{O}_2$  into  $\text{H}_2\text{O}$  and  $\text{O}_2$  leaving the oxide surface unchanged (reaction (1)) [2].

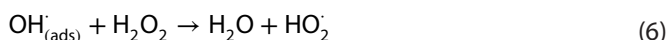


One oxide of particular importance under both reactor and nuclear waste repository conditions is  $\text{UO}_2$ . The reason for this is that most nuclear fuels used today are based on  $\text{UO}_2$ . Under anaerobic conditions, such as in groundwater at the depth of a geological repository for used nuclear fuel,  $\text{UO}_2$  has very low solubility and the radioactive fission products and heavier actinides produced during reactor operation are contained within the fuel matrix [3]. However, the inherent radioactivity of the fuel will induce radiolysis of the groundwater and subsequently production of oxidants capable of oxidizing the fuel matrix. The radiolytic oxidant of main importance in this process is  $\text{H}_2\text{O}_2$  and the release of radionuclides will be strongly dependent on competition between oxidation and catalytic decomposition [3]. It has previously been shown that for  $\text{UO}_2$  powder under certain conditions, about 80% of the hydrogen peroxide reacts via oxidation while the remaining 20% reacts via catalytic decomposition [4]. More recently, it was demonstrated that pressed and sintered  $\text{UO}_2$  pellets display a much higher ratio of catalytic decomposition [5–7]. The dissolution yield is defined as the amount of dissolved uranium divided by the amount of consumed hydrogen peroxide [4]. The dissolution yield has been demonstrated to decrease even more upon doping with rare earth metals serving as models for fission products [5, 6]. The decreased dissolution yield upon rare earth metal doping is mainly attributed to a reduced redox reactivity of the doped  $\text{UO}_2$  matrix [6]. However, the overall reactivity of the solid remains the same regardless of doping. The catalytic decomposition of  $\text{H}_2\text{O}_2$  on  $\text{UO}_2$ -based materials has also been studied using electrochemical techniques [8, 9].

The mechanism for catalytic decomposition of  $\text{H}_2\text{O}_2$  on metal oxide surfaces has been proposed to be the following [10, 11]:



This mechanism involves a redox cycling metal center. For the reaction between  $\text{H}_2\text{O}_2$  and  $\text{UO}_2$ , the rate determining step has been concluded to be one-electron transfer from the oxide to  $\text{H}_2\text{O}_2$  [12]. Catalytic decomposition of  $\text{H}_2\text{O}_2$  on other redox sensitive metal oxides has also been studied [13, 14]. For metal oxides where the metal is in its highest oxidation state, an alternative mechanism has been proposed [15]:



In this mechanism, the key-step is the homolysis of adsorbed  $\text{H}_2\text{O}_2$  producing adsorbed hydroxyl radicals.

The formation of hydroxyl radicals has been experimentally confirmed both for redox sensitive metal oxides like  $\text{UO}_2$  [6, 7] and for metal oxides where the metal is in its highest oxidation state (*e.g.*  $\text{ZrO}_2$ ) [16]. However, the detection of hydroxyl radicals cannot be used to distinguish between the two proposed mechanisms.

For  $\text{UO}_2$ -based materials the competition between oxidation of the  $\text{UO}_2$  matrix and catalytic decomposition has sometimes been assigned to two different types of surface sites [17]. In simulations of radiation-induced dissolution of spent nuclear fuel, a constant ratio between oxidation and catalytic decomposition is sometimes used to handle the competing reactions [18].

In this work, we have experimentally studied the competition between  $\text{UO}_2$  oxidation and catalytic decomposition of  $\text{H}_2\text{O}_2$  as a function of time and initial  $\text{H}_2\text{O}_2$  concentration. In view of the experimental results and previously published results, the mechanism of catalytic decomposition of  $\text{H}_2\text{O}_2$  on  $\text{UO}_2$  is discussed.

## 2. Experimental

### 2.1. Materials and sample preparation

The  $\text{UO}_2$  powder used in this study was provided by Westinghouse AB. The O/U ratio of the powder was determined to be 2.34. The O/U ratio was determined from the weight gain by oxidizing the powder to  $\text{U}_3\text{O}_8$  in air at 400 °C for 16 h. The oxidation to  $\text{U}_3\text{O}_8$  was confirmed by X-ray diffraction (XRD) (X'pert-Pro, PANalytical).

The specific surface area of  $\text{UO}_{2.34}$  was determined using the BET method of isothermal adsorption and desorption of a gaseous mixture consisting of 30%  $\text{N}_2$  and 70% He in a Micrometrics Flowsorb II 2300 instrument. The resulting specific surface area is  $5.4 \pm 0.2 \text{ m}^2/\text{g}$ .

### 2.2. Methods

The evolution of dissolved uranium and the concentration of  $\text{H}_2\text{O}_2$  as a function of reaction time have been measured by UV/VIS spectroscopy. Samples were filtered through a 0.20  $\mu\text{m}$  cellulose acetate syringe filter prior to photometric analysis. The arsenazo III method [19, 20]

(1,8-dihydroxynaphthalene-3,6-disulfonic acid-2,7-bis[(azo-2)-phenylarsonic acid]) has been used to determine the uranium concentration in solution at 653 nm while the Ghormley  $I_3^-$  method [21, 22] has been used to determine the  $H_2O_2$  concentration at 350 nm.

### 2.3. Dissolution experiments

Powder suspensions of  $UO_2$  (50 mg, 100 mg, and 200 mg) in  $1 \times 10^{-2} \text{ mol dm}^{-3} NaHCO_3$  were exposed to different concentrations of  $H_2O_2$  (0.2, 0.5, 1.0, 2.0, and  $5.0 \times 10^{-3} \text{ mol dm}^{-3}$ ). The total volume of the solutions was  $100 \text{ cm}^3$ .

The experiments were performed with continuous  $N_2$ -purging. All powders were washed three times in aqueous  $1 \times 10^{-2} \text{ mol dm}^{-3} NaHCO_3$  solution prior to the experiments.

## 3. Results and discussion

Four different concentrations of  $H_2O_2$  have been added to 100 mg powder suspensions containing  $1 \times 10^{-2} \text{ mol dm}^{-3} NaHCO_3$ . The reaction dynamics of the four batches were studied by measuring the concentrations of  $H_2O_2$  and U as a function of reaction time. The results are presented in Figure 1. As can be seen, the general behavior of the systems is similar to previous analogous studies [12, 23].

The kinetics of the reaction between  $UO_2$  and  $H_2O_2$  were analyzed by curve fitting. The kinetic evolutions of  $H_2O_2$  consumption and U dissolution were not explained by the single exponential function, indicating that the kinetics is not pseudo-first order. Therefore, both of the  $H_2O_2$  consumption and U dissolution were fit by multi-exponential function in order to obtain smooth curves for the kinetics,

$$c = A_0 + \sum_i^n A_i \exp(-k_i t) \quad (8)$$

where  $c$  denotes the concentration of  $H_2O_2$  or U,  $A_i$  and  $k_i$  were used as variable parameters and  $t$  is the reaction time. The results of fitting are shown in Figure 1. All the data-sets can be adequately expressed by Equation (8) with  $n \leq 3$ .

Using the smoothed curves, consumption rates of  $H_2O_2$  were calculated as the time derivatives of  $H_2O_2$  kinetics and shown in Figure 2. Each  $H_2O_2$  consumption rate for the different initial  $H_2O_2$  concentration decreased with decreasing  $H_2O_2$  concentration. However, the consumption rates for a given  $H_2O_2$  concentration were different depending on the initial  $H_2O_2$  concentration. For example, the  $H_2O_2$  consumption rate for  $2.0 \times 10^{-3} \text{ mol dm}^{-3}$  of initial  $H_2O_2$  was remarkably lower than the other cases when compared at the same  $H_2O_2$  concentration. Figure 2 clearly shows that the surface reactivity toward  $H_2O_2$  changes with turnover of  $H_2O_2$ . This is attributed to an alteration of the reactive interface, likely caused by blocking of surface sites by oxidized U/surface-bound hydroxyl radicals [15, 16, 24]. The initial  $H_2O_2$  consumption rate is plotted as a function of initial  $H_2O_2$  concentration in Figure 3. It is interesting to note that these four points display a slight curvature that could in fact be accounted for by the Freundlich adsorption isotherm. This would suggest that the initial  $H_2O_2$  consumption rate is proportional to the surface density of adsorbed  $H_2O_2$ .

As mentioned above, the dissolution yield of  $UO_2$  powder has been reported to be 80% [4], indicating that 80% of the  $H_2O_2$  is consumed to oxidize U(IV) to U(VI) and the remaining

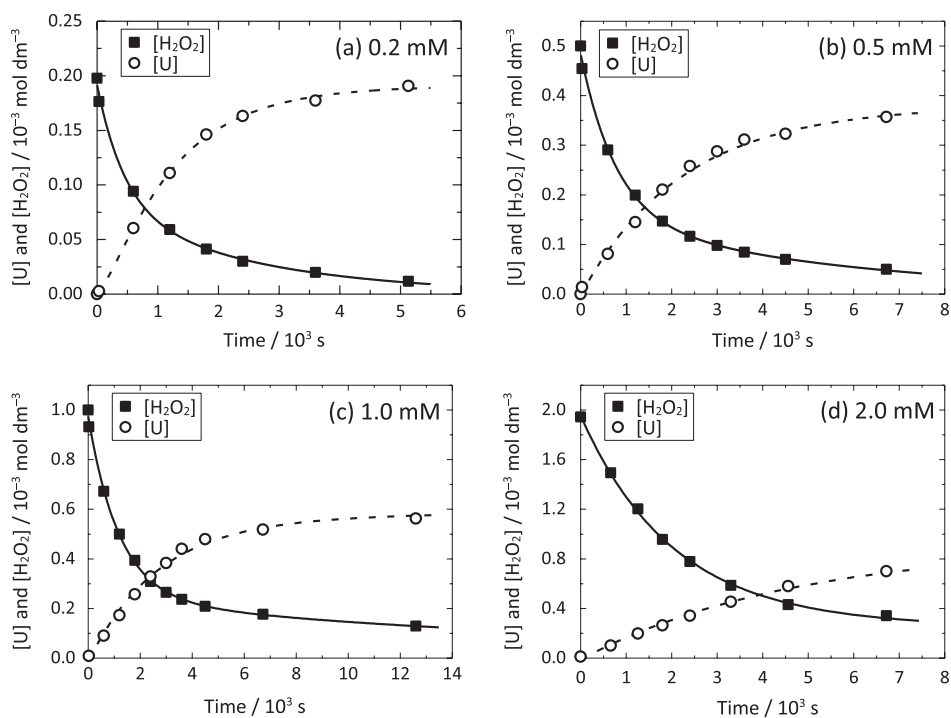


**Figure 1.** Curves fitted by multi exponential function, Equation (8), for the dissolution kinetics of  $\text{UO}_2$  with different initial concentrations of  $\text{H}_2\text{O}_2$ . (a)  $2 \times 10^{-4} \text{ mol dm}^{-3}$ , (b)  $5 \times 10^{-4} \text{ mol dm}^{-3}$ , (c)  $1 \times 10^{-3} \text{ mol dm}^{-3}$ , (d)  $2 \times 10^{-3} \text{ mol dm}^{-3}$ . The surface/volume used was  $5400 \text{ m}^{-1}$  ( $100 \text{ mg UO}_2$  in  $100 \text{ cm}^3$  of solution).

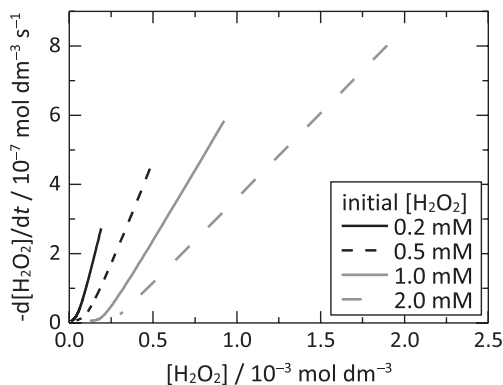


**Figure 2.** Reaction rates of  $\text{H}_2\text{O}_2$  for  $\text{UO}_2$  obtained as the first derivatives of fit curves shown in Figure 1.

20% undergoes catalytic decomposition on the  $\text{UO}_2$  surface. However, from the results in Figure 1 one can observe that the dissolution yield is not constant and appears to depend on the initial concentration of  $\text{H}_2\text{O}_2$ . This observation will be discussed in detail below.

The dissolution yield of uranium as a function of reaction time has been determined for the different systems presented above. The results are shown in Figure 4. As can be seen, the cumulative dissolution yield  $\left( \frac{[\text{UO}_{2(\text{aq})}^{2+}]_t}{[\text{H}_2\text{O}_2]_{\text{ini}} - [\text{H}_2\text{O}_2]_t} \right)$  increases with reaction time in all cases,

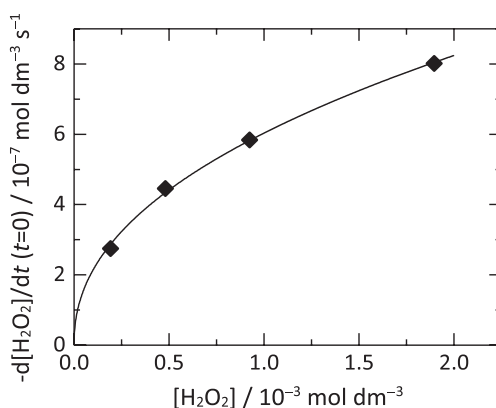


**Figure 3.** Initial reaction rates of H<sub>2</sub>O<sub>2</sub> as a function of H<sub>2</sub>O<sub>2</sub> concentration with a fit curve by power function,  $R_{in} = a c^{1/\eta}$ , where  $a$  and  $\eta$  are variable parameters.

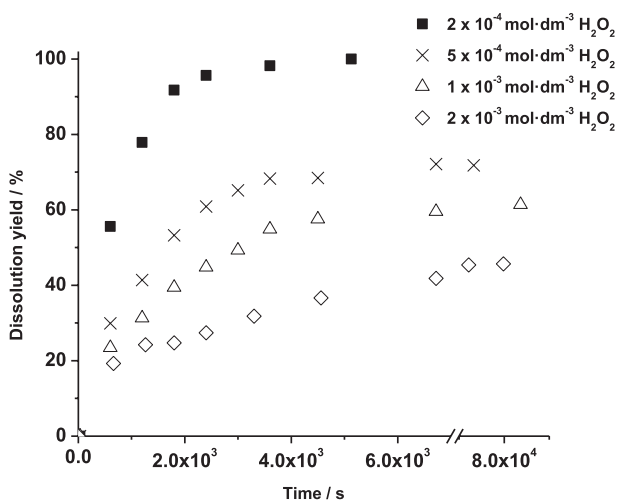


**Figure 4.** Cumulative dissolution yields of uranium as a function of reaction time. The surface/volume used was 5400 m<sup>-1</sup>.

displaying the well-known delay of uranium dissolution [12]. This delay in uranium dissolution is consistent with our interpretation of the decrease in surface reactivity caused by oxidized U/surface-bound hydroxyl radical. Contrary to what was implied in previous studies, the final dissolution yield is not constant and it is clear that it decreases with increasing initial concentration of H<sub>2</sub>O<sub>2</sub>.

The S/V ratio has been varied by exposing different amounts of UO<sub>2</sub> to different H<sub>2</sub>O<sub>2</sub> concentrations maintaining the same reaction volume. The final dissolution yields are summarized in Table 1. The results clearly show that the dissolution yield increases with decreasing initial concentration of H<sub>2</sub>O<sub>2</sub> for all three S/V ratios studied. Furthermore, the final dissolution yield for a given initial H<sub>2</sub>O<sub>2</sub> concentration does not differ significantly for the different S/V ratios used here.

**Table 1.** Final dissolution yields (%) for 50, 100, and 200 mg of  $\text{UO}_2$  in  $100 \text{ cm}^3$  ( $S/V = 2700, 5400, 10,800 \text{ m}^{-1}$ ) as a function of initial  $\text{H}_2\text{O}_2$  concentrations. The error associated to the results is  $\pm 2$ .

	$2 \times 10^{-4}$ $\text{mol dm}^{-3}$	$5 \times 10^{-4}$ $\text{mol dm}^{-3}$	$1 \times 10^{-3}$ $\text{mol dm}^{-3}$	$2 \times 10^{-3}$ $\text{mol dm}^{-3}$
50 mg	97	78	51	50
100 mg	100	72	61	46
200 mg	100	80	60	44

### 3.1. Mechanism

The strong  $\text{H}_2\text{O}_2$  concentration dependence of the dissolution yield provides some information about the nature of the hydroxyl radical formed in the first step of the catalytic decomposition of  $\text{H}_2\text{O}_2$ . Regardless of whether the first step of the catalytic  $\text{H}_2\text{O}_2$  decomposition on  $\text{UO}_2$  is electron transfer, Reaction (2), or homolysis, Reaction (5), hydroxyl radical is produced. Since  $\text{HCO}_3^-$  is a hydroxyl radical scavenger, with  $10 \text{ mM HCO}_3^-$  the free hydroxyl radical scavenging capacity is dominated by  $\text{HCO}_3^-$  in the whole  $\text{H}_2\text{O}_2$  concentration range. The fact that we still observe a strong  $\text{H}_2\text{O}_2$  concentration dependence implies that the relative reactivity of  $\text{HCO}_3^-$  and  $\text{H}_2\text{O}_2$  toward the hydroxyl radical is not that of the free hydroxyl radical. This change in reactivity compared to the homogeneous system implies formation of a surface-bound hydroxyl radical in the  $\text{UO}_2$  system. Further, the decrease in dissolution yield with increasing  $\text{H}_2\text{O}_2$  concentration implies competing reactions regarding the surface-bound hydroxyl radical between oxidation of surface U and scavenging by  $\text{H}_2\text{O}_2$ . As a direct consequence, the surface-bound hydroxyl radical must be regarded as a precursor for the oxidized metal. This precursor has a significant lifetime allowing the surface-bound hydroxyl radical to be scavenged.

The formation of a surface-bound hydroxyl radical on  $\text{UO}_2$  is also suggested by previous studies on the catalytic decomposition of  $\text{H}_2\text{O}_2$  on the surface of  $\text{UO}_2$ -based materials. There are studies on  $\text{UO}_2$ -based systems using Tris as hydroxyl radical scavenger [6, 7]. As for most other oxides, formaldehyde is detected indicating the formation of hydroxyl radicals. It should be noted that these experiments were performed in the presence of  $1\text{--}10 \text{ mM HCO}_3^-$  which, as stated above, is an efficient scavenger of free hydroxyl radicals in solution. Still, a significant amount of formaldehyde is formed in fair agreement with dissolution yields determined as the ratio between dissolved uranium and consumed  $\text{H}_2\text{O}_2$ . This is in line with the experiments presented above.

In the catalytic  $\text{H}_2\text{O}_2$  decomposition on metal oxides in their highest oxidation states (e.g.  $\text{ZrO}_2$ ), the formation of a surface-bound hydroxyl radical is more strongly supported by experiments [16, 25]. The catalytic decomposition of  $\text{H}_2\text{O}_2$  on such metal oxides is quantitatively converted to  $\text{O}_2$ . In the presence of some known hydroxyl radical scavengers, the  $\text{O}_2$  yield is reduced [26]. The reduction in  $\text{O}_2$  yield is proportional to the hydroxyl radical scavenger concentration [26]. Experiments using hydroxyl radical scavengers (mainly Tris and methanol) have been used to quantify hydroxyl radical production through the production of formaldehyde [25]. It has been shown that the formaldehyde yield (defined as the amount of formaldehyde produced per consumed amount of  $\text{H}_2\text{O}_2$ ) increases with increasing hydroxyl radical scavenger concentration and with decreasing  $\text{H}_2\text{O}_2$  concentration [25]. These trends can simply be accounted for by the competing reactions between hydroxyl radicals and  $\text{H}_2\text{O}_2$  on one hand and hydroxyl radicals and hydroxyl radical scavenger on the other hand.



This is very well in line with the mechanism proposed for catalytic decomposition of  $\text{H}_2\text{O}_2$ , which is expressed by reactions (5)–(7). This mechanism involves a surface-bound hydroxyl radical with a reactivity that is expected to be considerably lower than the reactivity of a free hydroxyl radical.

Interestingly, DFT calculations have shown that the activation barrier for catalytic decomposition of  $\text{H}_2\text{O}_2$  on metal oxide surfaces according to reactions (5)–(7) depends on the redox properties of the metal ion in the oxide [27]. According to the DFT calculations, the activation energy for reaction (5) increases with decreasing ionization potential of the metal ion in the oxide. The expected trend for the mechanism given by reactions (2)–(4) is the opposite, i.e. the activation energy for electron transfer (reaction (2)) is expected to decrease with increasing thermodynamic driving force of the reaction as has previously been observed for oxidation of  $\text{UO}_2$  [12]. For a given oxidant, the thermodynamic driving force increases with decreasing ionization potential of the metal ion in the oxide. The results of the present study indicate that the surface-bound hydroxyl radical can be formed also on the redox reactive  $\text{UO}_2$  surface. This could imply a gradual change from the mechanism given by reactions (2)–(4) toward the mechanism given by reactions (5)–(7) when going from easily oxidized metal oxides to metal oxides that are more difficult to oxidize.

## 4. Conclusion

On the basis of the experimental results and discussion presented above, we conclude the following:

- The initial rate of  $\text{H}_2\text{O}_2$  consumption on  $\text{UO}_2$  is governed by adsorption.
- Alteration of the reactive interface as a consequence of the reaction between  $\text{H}_2\text{O}_2$  and  $\text{UO}_2$ , likely caused by blocking of surface sites by oxidized U/surface-bound hydroxyl radicals, reduces the rate of the reaction.
- The hydroxyl radical produced as an intermediate in the catalytic decomposition of  $\text{H}_2\text{O}_2$  on  $\text{UO}_2$  is surface bound. In the absence of a radical scavenger, like  $\text{H}_2\text{O}_2$ , the surface-bound hydroxyl radical results in surface oxidation.

## Acknowledgements

The Swedish Nuclear Fuel and Waste Management Co., SKB AB, is gratefully acknowledged for financial support.

## Disclosure statement

No potential conflict of interest was reported by the authors.

## References

- [1] J.W.T. Spinks, R.J. Woods. *An Introduction to Radiation Chemistry*, 3rd Edn., John Wiley & Sons, New York, NY (1990).
- [2] F. Haber, *J. Weiss. Proc. Royal Soc. A*, **147**, 332 (1934).
- [3] D.W. Shoesmith. *J. Nucl. Mater.*, **282**, 1 (2000).
- [4] M. Jonsson, E. Ekeröth, O. Roth. *MRS Proc.*, **807**, 77 (2004).

- [5] S. Nilsson, M. Jonsson. *J. Nucl. Mater.*, **410**, 89 (2011).
- [6] R. Pehrman, M. Trummer, C.M. Lousada, M. Jonsson. *J. Nucl. Mater.*, **430**, 6 (2012).
- [7] C.M. Lousada, M. Trummer, M. Jonsson. *J. Nucl. Mater.*, **434**, 434 (2013).
- [8] J.S. Goldik, H.W. Nesbitt, J.J. Noël, D.W. Shoesmith. *Electrochim. Acta*, **49**, 1699 (2004).
- [9] J.S. Goldik, J.J. Noël, D.W. Shoesmith. *J. Electrochem. Soc.*, **153**, E151 (2006).
- [10] N. Kitajima, S.-I. Fukuzumi, Y. Ono. *J. Phys. Chem.*, **82**, 1505 (1978).
- [11] J. Weiss. *Trans. Faraday Soc.*, **31**, 1547 (1935).
- [12] E. Ekeröth, M. Jonsson. *J. Nucl. Mater.*, **322**, 242 (2003).
- [13] S.-S. Lin, M.D. Gurol. *Environ. Sci. Technol.*, **32**, 1417 (1998).
- [14] D. Fu, X. Zhang, P.G. Keech, D.W. Shoesmith, J.C. Wren. *Electrochim. Acta*, **55**, 3787 (2010).
- [15] A. Hiroki, J.A. LaVerne. *J. Phys. Chem. B*, **109**, 3364 (2005).
- [16] C.M. Lousada, M. Jonsson. *J. Phys. Chem. C*, **114**, 11202 (2010).
- [17] T.E. Eriksen, M. Jonsson, J. Merino. *J. Nucl. Mater.*, **375**, 331 (2008).
- [18] N. Liu, L. Wu, Z. Qin, D.W. Shoesmith. *Environ. Sci. Technol.*, **50**, 12348 (2016).
- [19] I.K. Kressin. *Anal. Chem.*, **56**, 2269 (1984).
- [20] S.B. Savvin. *Talanta*, **8**, 673 (1961).
- [21] J.A. Ghormley, A.C. Stewart. *J. Am. Chem. Soc.*, **78**, 2934 (1956).
- [22] C.J. Hochanadel. *J. Phys. Chem.*, **56**, 587 (1952).
- [23] M. Trummer, B. Dahlgren, M. Jonsson. *J. Nucl. Mater.*, **407**, 195 (2010).
- [24] M. Suh, P.S. Bagus, S. Pak, M.P. Rosynek, J.H. Lunsford. *J. Phys. Chem. B*, **104**, 2736 (2000).
- [25] M. Yang, M. Jonsson. *J. Mol. Catal. A: Chem.*, **400**, 49 (2015).
- [26] C.M. Lousada, J.A. LaVerne, M. Jonsson. *Phys. Chem. Chem. Phys.*, **15**, 12674 (2013).
- [27] C.M. Lousada, T. Brinck, M. Jonsson. *Comput. Theor. Chem.*, **1070**, 108 (2015).